Sliding-Mode Control of Nonlinear Discrete-Input Pneumatic Actuators

Sean Hodgson[1], Minh Quyen Le[2], Mahdi Tavakoli[1], Minh Tu Pham[2]

[1]Department of Electrical and Computer Engineering, University of Alberta, Edmonton, AB Canada T6G2V4

[2]Laboratoire Ampère, UMR CNRS 5005, Université de Lyon, INSA-LYON, F-69621 Villeurbanne Cedex, France

Abstract— This paper proposes a sliding mode law for precise position control with minimal switching activity for a robotic system that uses on/off (solenoid) pneumatic actuators, For a two-chamber pneumatic actuator with four binary solenoid valves, there is a total of sixteen possible input combinations defined directly from the state of the four on/off solenoid valves present in the system. However, only seven of these discrete operating modes are considered both functional and unique. Accordingly, we use a seven-mode sliding controller that minimizes the position error using modes that have both the necessary and sufficient amounts of drive energy and, thus, involve reduced switching activity. An analysis of the closed-loop system stability is carried out. The performance of the proposed control design is experimentally verified on a single pneumatic actuator comprising of two chambers driven by four on/off solenoid valves.

Index Terms— Pneumatic actuator, on/off solenoid valve, robot control, sliding mode control, position tracking, switching activity, stability.

I. Introduction

Recent developments in robotics and telerobotics have allowed working in environments that are normally difficult or hazardous for the human hand to reach or operate in. Robotic systems have been developed for applications ranging from surgery to space exploration. In robot-assisted surgery, for instance, robots may be required to work in areas that have strong magnetic fields. Magnetic Resonance Imaging (MRI) affords images with high resolution and contrast and allows surgeons to access a patient's three-dimensional visualization in real-time [1].

Pneumatic actuators offer many advantages for positioning applications in addition to being inert to magnetic fields: low maintenance cost, high ratio of power to weight, cleanliness and safety are some of these advantages [2]. However, they suffer from common drawbacks including friction and sensitivity of actuator dynamics to load and piston position along the cylinder stroke [3]. Also, from a control perspective, controlling a pneumatic actuator is a challenge because the system dynamics are highly non-linear [4].

The non-linear nature of a pneumatics actuator is exacerbated when it uses on/off solenoid valves, which have wide-spread applications due to the high cost of servo-valves (due to the precision machining required in their manufacturing) [5]. In this case, precise control is difficult due to the discrete-input nature of the system. Most solenoid-valve pneumatic systems utilize a pulse width modulated (PWM) controller. Using time averaging, a PWM input with a sufficiently high frequency can approximate the continuous input properties of a servo-valve [6]. Regardless of whether
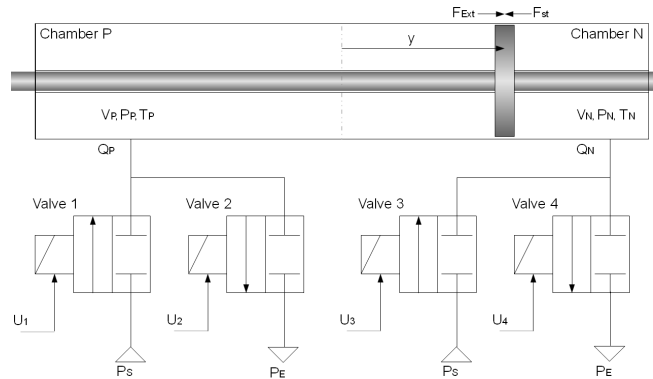

Fig. 1. Electro-pneumatic system with 4 on/off solenoid valves

a servo-valve or PWM input is utilized, a control method must be chosen to compensate for the non-linearities of the system. In [2] the nonlinear system is transformed into an equivalent linear system (controlled by PWM). Because of the highly nonlinear nature of a pneumatic system it is better to address its control with a nonlinear model based control. Other research areas use non-linear averaging techniques based on a sliding mode approach to control pneumatic systems [3], [4], [6], [7].

Sliding mode control is a form of variable structure control that alters the dynamics of a nonlinear system by the application of a high-frequency switching control [8]. Sliding mode control can account for the non-linearities of the system as well as its dynamic uncertainties [5]. In this paper we consider a pneumatic actuator comprised of two chambers as shown in Figure 1. Each chamber has two solenoid valves, each of which can be either locked or connected to a compressed air supply (source pressure) or to exhaust (atmosphere pressure). Since we cannot have a chamber connected to both pressure and exhaust at the same time, only nine discrete modes exist. We assume the three modes where both chambers are locked, venting, and pressurizing are functionally equivalent, then we can assume the system has a total of seven unique discrete modes.

The sliding control system utilizes discrete operating modes defined directly from the state of the on/off solenoid valves, with the switching between these discrete modes decided based on the current tracking error, thereby bypassing the need for a PWM input. In [5], three discrete modes are considered for a two-chamber actuator (see Figure 1): two modes defined by connecting one chamber to exhaust and connecting one chamber to pressure (and the reverse thereof)

and one mode defined by closing all valves.

In this paper, we expand the three-mode open-loop model of [5] into a seven-mode open-loop model. The new system has four extra modes defined by opening only one of the four solenoid valves at a time, which facilitate appropriate amounts of drive energy for good positioning precision and reduced switching activity.

Limiting the drive power allows us to make smaller and fewer adjustments, improving the positioning accuracy of the controlled system. Compared to the 3 mode paper we are extending to 7 modes and providing guidelines for the parameters τ, β and ϵ, which will be discussed later.

We will decide the thresholds for transition from one control mode to another control mode based on the full state of the system: piston position, velocity, and acceleration as well as chamber pressures. By optimizing these transition thresholds, we can decrease the open-close activity of the on/off solenoid valves, which increases their operating lifespan.

The organization of this paper is as follows: The modeling of the pneumatic actuator with its chamber and 4 solenoid valves is reported in Section II. The discrete input model of the actuator is given in Section III. The design and theoretical analysis of the sliding controller are discussed in Section IV. The simulation study to verify the control laws are presented in this paper in Section V The experimental results are presented in this paper in Section VI. Finally, the concluding remarks are presented in Section VII.

II. MODELING OF THE OPEN-LOOP PNEUMATIC ACTUATOR

This section of the paper derives the open-loop model of the pneumatic actuator including its on/off solenoid valves as shown in Figure 1. To describe the air flow dynamics in a cylinder, we assume that: Air is a perfect gas and its kinetic energy is negligible in the chamber, the pressure and the temperature are homogeneous in each chamber, the evolution of the gas in each chamber is polytropic, with the exception of some controller thresholds which were selected using isothermic assumptions. The temperature variation in chambers is negligible with respect to the supply temperature. The mass flow rate leakages are negligible, and the supply and exhaust pressures are constant.

The Simscape simulations in Section V does not assume/model all of these assumptions.

A. Model of the Pneumatic Chambers

If the charging and discharging of the chambers' cylinders are assumed to be polytropic, then the pressure dynamics of these chambers can be approximated [9] as

$$\dot{P}_P = \frac{k}{V_P}(rTQ_P - AP_P\dot{y}) \qquad \dot{P}_N = \frac{k}{V_N}(rTQ_N + AP_N\dot{y})$$

$$(1)$$

where P_P and P_N refer to pressures (Pa) inside the chambers P and N, respectively, V_P and V_N refer to volumes (m³) of the chambers P and N, respectively, Q_P and Q_N refer to

mass flow rates (kg/s) of the chambers P and N, respectively, A refers to the piston cylinder area (m²), T refers to the chamber temperature (K), k refers to the polytropic constant, r refers to the universal gas constant (J/(kgK)), and y refers to the piston position (m) shown in Figure 1. Note the arrows for position y, Force (N) F_{Ext} and F_{st} shown in Figure 1 refer to their positive directions, a negative magnitude to any of these quantities will refer to the opposite direction.

B. Model of the valves

The mass flow rates Q_P and Q_N can be derived in terms of the discrete voltage inputs U_1, U_2, U_3 and U_4 shown in Figure 1 and the continuous pressure inputs P_P and P_N:

$$Q_P = U_1 Q(P_S, P_P) - U_2 Q(P_P, P_E) \qquad (2a)$$

$$Q_N = U_3 Q(P_S, P_N) - U_4 Q(P_N, P_E) \qquad (2b)$$

Here, P_S and P_E are the pressures of the supply and the exhaust. In general, $Q(P_{Up}, P_{Down})$ used in (2a) and (2b), in which P_{Up} is the upstream pressure and P_{Down} is the downstream pressure, refers to the expression for the mass flow rate through an orifice. This generalized model has two parameters to describe the mass flow rate: the critical pressure ratio $b = 0.433$ and the sonic conductance C_{val} (mass flow rate constant) [10]:

$$Q(P_{Up}, P_{Down}) = C_{val} P_{Up} \sqrt{\frac{T_{Atm}}{T_{Up}}} \times$$

$$\begin{cases} \sqrt{1 - \left(\frac{\frac{P_{Down}}{P_{Up}} - b}{1 - b}\right)^2} & \text{, if } \frac{P_{Down}}{P_{Up}} > b \text{ (subsonic)} \\ 1 & \text{, if } \frac{P_{Down}}{P_{Up}} \le b \text{ (choked)} \end{cases} \quad (3)$$

In the above, T_{Up} is the upstream temperature of air and T_{Atm} is the atmospheric temperature. Also, C_{Val} is a characteristic of the valve.

C. Model of the Piston

Finally, the dynamics of the mechanical actuator involving the applied force on the piston and the resulting piston motion is

$$A(P_P - P_N) - b_m\dot{y} + F_{Ext} - F_{St} = M_m\ddot{y} \qquad (4)$$

where b_m is the viscose coefficient (N s/m)), M_m is the total mass of the load and the piston (Kg), F_{St} is the stiction force (N), and F_{Ext} is the external force (N). For simplicity, the stiction force and external force is assumed to be negligible. The F_{St} was considered to be negligible since the pneumatic actuator used in experiment was an Airpel anti-stiction cylinder (ALL AIR Inc, New York, US).

III. DISCRETE INPUT MODEL OF THE OPEN-LOOP ACTUATOR

It is possible to combine the equations in Section II to write the dynamics of the open-loop pneumatic actuator in a 7-mode discrete-input. Differentiating (4) and substituting

(1) in it, the dynamics of the actuator are obtained as

$$\ddot{y} = F(Z) + \frac{krT}{M_m}\left(\frac{Q_P}{l/2+y} - \frac{Q_N}{l/2-y}\right) \tag{5}$$

where $Z = \{y, \dot{y}, \ddot{y}, P_P, P_N\}$ is the state vector and

$$F(Z) = \frac{-b_m}{M_m}\ddot{y} - \frac{Ak}{M_m}\left(\frac{P_P}{l/2+y} + \frac{P_N}{l/2-y}\right)\dot{y}$$

where l is the total length of the chamber. We find that there are a total of nine discrete modes for the solenoid valves [9]. These modes are shown in Table I. This paper will outline a controller that only utilizes modes M_1 through M_7 of the open-loop system. For the seven discrete modes, dynamic

TABLE I

NINE DISCRETE MODES OF THE OPEN-LOOP ACTUATOR

	M_1	M_2	M_3	M_4	M_5	M_6	M_7	M_8	M_9
U_1	0	1	0	0	0	1	0	0	1
U_2	0	0	1	0	0	0	1	1	0
U_3	0	0	0	0	1	0	1	0	1
U_4	0	0	0	1	0	1	0	1	0

equation can be obtained by substituting (2a) and (2b) into (5). We obtain

$$\ddot{y} = \begin{cases} F(Z) & , \text{mode } M_1 \\ F(Z) + (-1)^i B_i(Z) & , \text{mode } M_i \neq M_1 \end{cases} \tag{6}$$

$$B_2(Z) = \frac{krT}{M_m}\frac{Q(P_S, P_P)}{(l/2+y)} \qquad B_3(Z) = \frac{krT}{M_m}\frac{Q(P_P, P_E)}{(l/2+y)}$$

$$B_4(Z) = \frac{krT}{M_m}\frac{Q(P_N, P_E)}{(l/2-y)} \qquad B_5(Z) = \frac{krT}{M_m}\frac{Q(P_S, P_N)}{(l/2-y)}$$

$$B_6(Z) = B_2(Z) + B_4(Z) \qquad B_7(Z) = B_5(Z) + B_3(Z)$$

Note that because $P_E \leq P_P \leq P_S$, $P_E \leq P_N \leq P_S$ and $-l/2 \leq y \leq l/2$ and mass flow rates are non-negative functions $B_2(Z)$ through $B_7(Z)$ are all positive or equal to zero. The value i takes a range of integer values from 2 to 7.

IV. THE SLIDING MODE CONTROLLER DESIGN

For a position-controlled system, we can define the following sliding surface $s = 0$ where s is defined as:

$$s = \frac{\ddot{e}}{\omega^2} + \frac{2\xi\dot{e}}{\omega} + e \tag{7}$$

where e is the position error $y - y_d$, y is the actual position, y_d is the desired position, and ξ and ω are constant and positive numbers. We use this function s and invoke the seven different modes of the open-loop system based on five different regions of the function s. These regions of s and the selected operating mode of the system are illustrated in Table II. Please note that the input voltages (i.e., control actions) for each mode is listed in Table I.

TABLE II

SELECTION OF THE OPERATING MODE BASED ON POSITIONING ERROR s

Region	Discrete operating modes	Magnitude of $\dot{s}$ from (10)
$s > \beta$	M_7	Large negative
$\beta \geq s > \epsilon$	M_3 and M_5	Modest negative
$\epsilon \geq s > -\epsilon$	M_1	Minimal
$-\epsilon \geq s > -\beta$	M_2 and M_4	Modest positive
$-\beta \geq s$	M_6	Large positive

A. Stability

To be able to analyze stability, consider the Lyapunov function candidate

$$V = \frac{1}{2}s^2 \tag{8}$$

V is a positive-valued function, therefore if $\dot{V} < 0$, V and $|s|$ will be decreasing. Assuming s is initially bounded, s will asymptotically approach zero if we control the system so that

$$\dot{V} = \dot{s}s < -\eta|s| \tag{9}$$

for some constant $\eta > 0$ [8][5]. Take the derivative of (7) and substitute (6) to obtain

$$\dot{s} = \begin{cases} \lambda & , mode\ M_1 \\ \lambda + (-1)^i B_i(Z)/\omega^2 & , mode\ M_i \neq M_1 \end{cases} \tag{10}$$

where $\lambda = (F(Z) - \ddot{y}_d)/\omega^2 + 2\xi\ddot{e}/\omega + \dot{e}$. λ will be bounded if $\dot{y}$, $\ddot{y}$, $\dot{y}_d$, $\ddot{y}_d$, $\dddot{y}_d$, P_P and P_N are bounded. P_P and P_N are bounded between P_S and P_E. y_d is a controlled input to the system thus y_d, $\dot{y}_d$, $\ddot{y}_d$, $\dddot{y}_d$ are assumed to be bounded. If we rewrite the (4) as

$$M_m\ddot{y} + b_m\dot{y} = A(P_P - P_N) \tag{11}$$

we see that the right side of (11) is always bounded. Therefore velocity is a 1st order differential equation, which means velocity is a decaying exponential. Therefore if $\dot{y}$ is initially bounded, then $\dot{y}$ will always be bounded. If we rewrite (4)

$$\ddot{y} = \frac{1}{M_m}(A(P_P - P_N) - b_m\dot{y}) \tag{12}$$

We find that it is defined purely in terms of bounded functions, thus it too must always be bounded. Therefore λ is also bounded.

Therefore if the positive-valued functions $B_i(Z)$ are sufficiently large then modes M_2, M_4 and M_6 can ensure $\dot{s} > \eta$ and the modes M_3, M_5 and M_7 can ensure $\dot{s} < -\eta$.

All six functions $B_i(Z)$ are linearly proportional to C_{val} and P_S, the valve's mass flow rate constant in (3), thus choosing a large enough valve or supply pressure will ensure that these scalar functions will be sufficient in magnitude. Thus, using the modes M_2, M_4 and M_6 when $s < 0$, and using M_3, M_5 and M_7 when $s > 0$. Will ensure (9), and thus the convergence of s to zero over time.

if s converges to zero and y_d, $\dot{y}_d$, $\ddot{y}_d$ are bounded the

output y, $\dot{y}$, $\ddot{y}$ will also be bounded and thus the system will be BIBO stable.

B. Controller Mode Selection

The 7-mode controller requires knowledge of the current chamber pressures to pick the appropriate operating modes. This requires additional sensors as compared to the 3-mode controller. These sensors are required for deciding which control mode to use when $\beta \geq |s| > \epsilon$ (see Table II).

We will first study the negative region $-\beta \geq s > -\epsilon$, if we evaluate (4) under mode M_2 and assume that the filling chamber has a sufficient amount of time to be fully pressurized we can see that the $\ddot{y} \propto (P_S - P_N)$. If we evaluate (4) under mode M_4 and assume that the venting chamber has a sufficient amount of time to be fully vented we can see that the $\ddot{y} \propto (P_P - P_E)$ If we define

$$
\begin{aligned}
E_1 &= (P_S - P_N) - (P_P - P_E) \\
&= (P_S + P_E) - (P_P + P_N) \quad (13)
\end{aligned}
$$

the magnitude of E_1 is positive when the pressure difference $P_S - P_N$ is greater than the pressure difference $P_P - P_E$. Therefore, when E_1 is positive, the appropriate operating mode for the region $-\epsilon \geq s > -\beta$ is M_2 as it will result in a higher piston acceleration compared to the mode M_4. Conversely when the magnitude of E_1 is negative M_4 will result in a higher piston acceleration compared to M_2. In the positive region $\beta \geq s > \epsilon$, comparing modes M_5 and M_3, from (4) we see that the magnitudes of $\ddot{y}$ are based on the pressure differences $P_S - P_P$ and $P_N - P_E$ respectively. Let us define

$$
E_2 = (P_S - P_P) - (P_N - P_E) = E_1 \quad (14)
$$

The magnitude of E_2 is positive when the pressure difference $P_S - P_P$ is greater then the pressure difference $P_N - P_E$. Therefore when E_2 is positive the appropriate operating mode for the region $\epsilon \geq s > \beta$ is M_5 as it will accelerate the piston more compared to mode M_3. Conversely when the magnitude of E_2 is negative mode M_3 will result in a higher piston acceleration compared to M_5 In summary, the magnitude of s in (7) and the magnitude of E_1 in (13) can be used by the controller to select the best of the seven operating modes see Figure 2.

C. Selecting Parameters τ, β and ϵ

This section proposes appropriate ways for selecting the controller parameters of τ, β and ϵ for smoothest motions and least switching activity.

1) Selecting τ: The purpose of the timeout parameter τ is to reduce switching between the modes used in the region $\beta \geq |s| > \epsilon$ by enforcing a minimum amount of time between modes transitions in this region. A larger τ value will reduce switching. A smaller τ value will give a more accurate output. There is a trade-off between these goals, therefore an appropriate value of τ should be determined by evaluating the open-loop responses M_2 and M_4. For initial conditions (at $t = 0$) of $y = 0$ and $V_P = V_N = A\frac{l}{2}$ (i.e., the piston positioned in halfway along the cylinder length), using
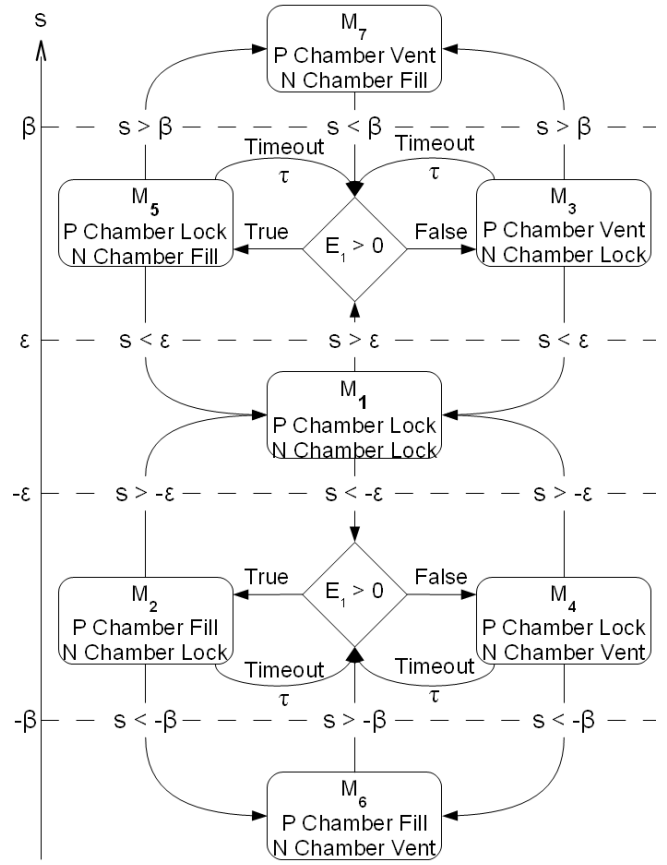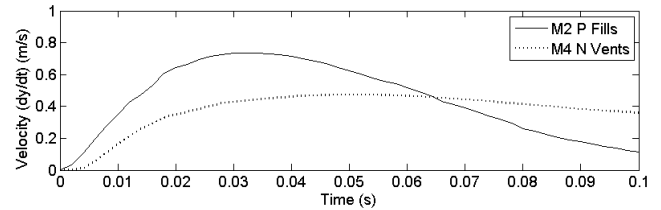

Fig. 2.   7-mode controller diagram

Fig. 3.   Open-loop responses modes M_2 and M_4

(1) - (4) we can simulate the open-loop system response in each of these modes (Figure 3). These initial conditions where selected because they are symmetric in nature.

For the pressurizing case M_2 the intial conditions $P_P = P_N = P_E$ was selected. For the venting case M_4 the intial conditions $P_P = P_N = P_S$ was selected.

We define t_{fill} as the time it takes to reach the maximum velocity $\max(\ddot{y})$ for the M_2 Chamber P filling profile and t_{vent} as the time it takes to reach the maximum velocity $\max(\ddot{y})$ for the M_4 Chamber N venting profile. If we compare t_{fill} and t_{vent} obtained from simulation we see that t_{fill} is a shorter span of time. For our system tests we have selected $\tau = t_{fill}$.

2) Selecting β: The magnitude β is the transition threshold between a mode connecting the two chambers to supply and exhaust pressures (i.e., M_6 or M_7), and the alternating modes for opening only a single valve (i.e., M_2/M_4 or

M_3/M_5).

For our purposes β was chosen empirically. We used the following equation as a starting point.

$$\beta = \frac{3A(P_S - P_E)}{8\omega b_m} \qquad (15)$$

A higher β was found to be more optimal for y_{ref} signals with large variation and a smaller β was found to be more optimal for y_{ref} signals with smaller variation.

For our experiments the we selected a β = 3mm. This selection of β is not unique however it has been demonstrated in our results as being appropriate.

3) Selecting ϵ: When the magnitude of s is less than a positive valued but small ϵ, the controller removes the actuation from the system by closing all valves. The magnitude of ϵ should ideally be selected so that when this occurs and the effect of past actuations settles out, the position difference, $y - y_d$, will be less than some desired small amount e_{min}. Therefore, ϵ is selected as $\epsilon = e_{min}$

V. SIMULATION STUDY

To analyze the performance of the 7-mode controller described in this paper we will be comparing it against the original 3-mode controller it was based on in [5].

A. Simulation Parameters and Test Inputs

For our simulation, we selected the model parameters listed in Table III. These model parameters correspond to the experimental setup that will be used in Section VI. The

TABLE III
SYSTEM PARAMETERS TABLE

Var.	Value	Label
l	0.1m	Chamber Length
T	23 C	Chamber Temperature
C_{val}	3.4×10^{-9} kg/(s Pa)	Mass Flow Rate Const.
P_S	$300,000$ Pa	Supply Air Pressure
P_E	$100,000$ Pa	Exhaust Air Pressure
k	1.2	polytropic constant
A	1.814 cm^2	Piston Cylinder Area
b_m	50 (N s)/m	Viscosity Coefficient
M_m	0.9 kg	Total Mass of load

following controller parameters were selected: ω = 100 rad/s, ξ = 0.5, τ = 40ms, β = 3mm and ϵ = 1mm. To model our system we utilized the Simulink Simscape toolbox.

B. Simulation Results

The simulation was run utilizing a 40mm peak-peak sine wave test input with frequencies varying from 0.1Hz - 3.0Hz, the results of the simulations are charted in Figure 4. From these results, we find that for both the 3-mode and the 7-mode systems increasing the input frequency leads to an increasing RMS tracking error

In the 7 mode system, for moderate differences between y_d and y, this difference may not be enough to switch from the $|s| > \beta$ region. As we can see this can cause an
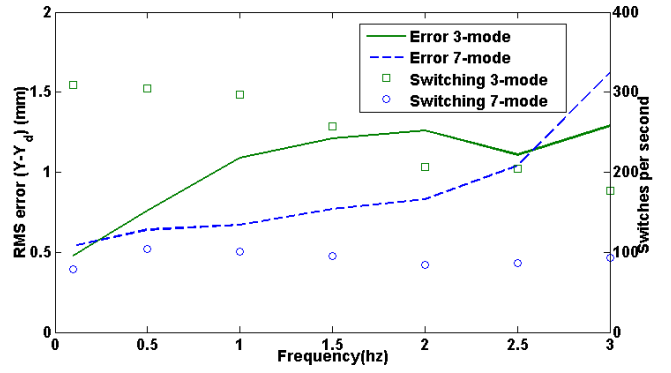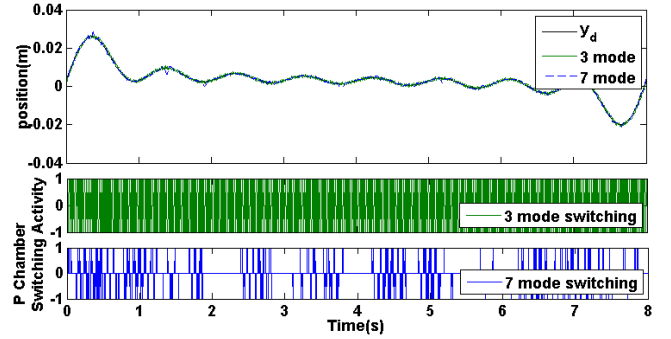

Fig. 4.   Sine-wave simulation results

Fig. 5.   Multiple summed sine-wave simulation results

increase in tracking error in the 2-3hz range for the 7-mode system. This is one of the costs of using the 7-mode sliding control algorithm. The advantage of the 7-mode controller algorithm is the reduction in the solenoid valves switching as observed in Figure 4. At 1.5Hz, this is equal to 63% reduction in switching activity and 0.45mm improvement in tracking error.

To test the system with a more complicated signal, we used an input that is a summation of 8 sine waves with 8 different frequencies. As we can see from Figure 5, both controllers have no trouble tracking the multi-sine wave; however the switching activity for the 7-mode controller is greatly reduced compared to the 3-mode controller. From the 3-mode controller to the 7-mode controller, there is a 64% reduction in solenoid switching activity.

VI. EXPERIMENTAL TESTING

In this section, experiments with a 1-DOF system are reported. This experimental setup is the same as the one described in [11] for a single actuator. For this experiment, the following controller parameters were selected were the same as in simulation except ω = 60 rad/s.

A. Experimental Results

The experiment was run utilizing a 40mm peak-peak sine wave test input with frequencies varying from 0.1Hz - 3.0Hz. The recorded results from these experiments are charted in Figure 6. When we compare these results for the 3-mode controller and the 7-mode controller, we can see that there
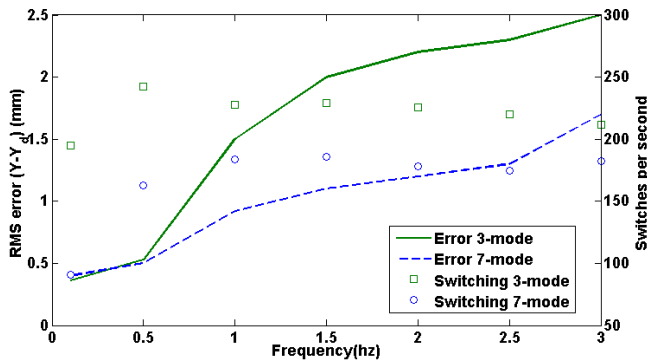
Fig. 6. Sine-wave experimental results

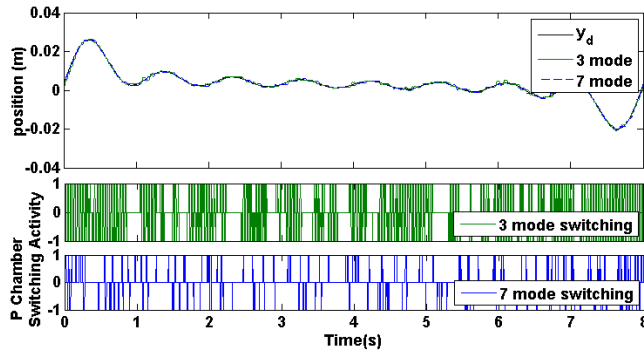Fig. 8. Sine Wave 1.5Hz with 1kg load attached to actuator

Fig. 7. Multiple summed sine-wave experimental results

was a notable improvement to tracking performance and switching activity for the 7-mode controller (compared to the 3-mode controller).

To test the system with a more complicated signal, we used an input that is a summation of 8 sine waves with 8 different frequencies (exact same as in simulation). As we can see from Figure 5, both controllers have no trouble tracking the multi-sine wave; however the switching activity for the 7-mode controller is reduced compared to the 3-mode controller. From the 3-mode controller to the 7-mode controller, there is a 49% reduction in solenoid switching activity.

To test the load disturbance rejection of the algorithm a 1kg weight was attached to the actuator using a rope and a pulley. The experiment was run utilizing the sine wave test input with a 1.5Hz frequency. The recorded results are shown in Figure 8. Tracking error for both 3 mode and 7 mode increased by 0.2mm RMS. Switching was found to increase for both 3 mode and 7 mode by $\sim 10\%$.

VII. CONCLUDING REMARKS

This paper proposed a sliding mode law for precise position control with minimal switching activity designed for use on a pneumatic actuator. The two-chamber actuator with four on/off solenoid valves had a total of sixteen possible modes only seven of which were considered functional and unique and were used for this particular control law. This controller uses four more additional modes compared to [5] that decrease the coarseness in the drive force for lower
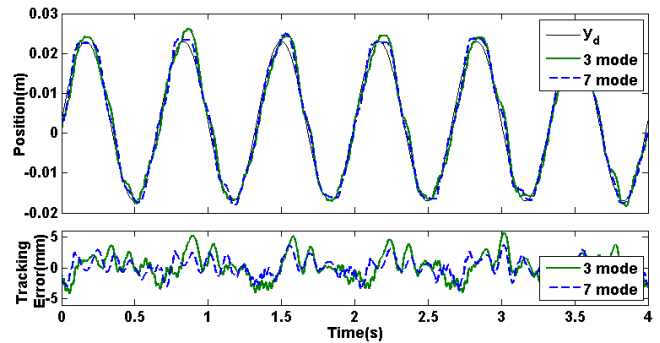
position tracking errors. The main advantage of the 7-mode controller is a reduction in the switching of the solenoid valves compared to the 3-mode control. The tracking error performance was experimentally found to improve in 7-mode as compared to 3-mode control.

REFERENCES

[1] M. Oura, Y. Kobayashi, J. Okamoto, and M. Fujie, "Development of MRI compatible versatile manipulator for minimally invasive surgery," in *Proceedings of 2006 First IEEE/RAS-EMBS International Conference on Biomedical Robotics and Biomechatronics (BIOROB)*, Tuscany, Itally, Febuary 2006, pp. 176–181.

[2] J. A. Rosas-Flores, J. A. Flores-Campos, and L. G. Corona-Ramírez, "Optimal linearization of the dynamic behavior of an on/off actuated single pneumatic cylinder," in *Proceedings of 2008 5th International Conference on Electrical Engineering, Computing Science and Automatic Control (CCE 2008)*, Mexico City, November 2008, pp. 380–385.

[3] A. Girin, F. Plestan, X. Brun, and A. Glumineau, "High-order sliding-mode controllers of an electropneumatic actuator: Application to an aeronautic benchmark," *International Journal of Control*, vol. 79, no. 2, pp. 119–131, 2006.

[4] K. Xing, J. Huang, Y. Wang, J. Wu, Q. Xu, and J. He, "Tracking control of pneumatic artificial muscle actuators based on sliding mode and non-linear disturbance observer," *IET Control Theory and Applications*, vol. 4, no. 10, pp. 2058–2070, 2010.

[5] T. Nguyen, J. Leavitt, F. Jabbari, and J. E. Bobrow, "Accurate sliding-mode control of pneumatic systems using low-cost solenoid valves," *IEEE/ASME Transactions on Mechatronics*, vol. 12, no. 2, pp. 216–219, 2007.

[6] X. Shen, J. Zhang, E. J. Barth, and M. Goldfarb, "Nonlinear model-based control of pulse width modulated pneumatic servo systems," *Journal of Dynamic Systems, Measurement, and Control*, vol. 128, pp. 663–669, 2006.

[7] M. Q. Le, M. T. Pham, M. Tavakoli, and R. Moreau, "Sliding mode control of a pneumatic haptic teleoperation system with on/off solenoid valves," in *Proceedings of IEEE International Conference on Robotics and Automation (ICRA)*, Shanghai, China, May 2011, pp. 874–879.

[8] V. Utkin, "Sliding mode control design principles and applications to electric drives," *IEEE Transactions on Industrial Electronics*, vol. 40, no. 1, pp. 23–36, 1993.

[9] M. Q. Le, M. T. Pham, R. Moreau, and T. Redarce, "Transparency of a pneumatic teleoperation system using on/off solenoid valves," in *Proceedings of 19th IEEE International Symposium on Robot and Human Interactive Communication (RO-MAN)*, Viareggio, Italy, September 2010, pp. 15–20.

[10] P. Beater, *Pneumatic Drives - System Design, Modelling and Control*. Berlin: Springer, 2006.

[11] M. Q. Le, M. T. Pham, M. Tavakoli, and R. Moreau, "Development of a hybrid control for a pneumatic teleoperation system using on/off solenoid valves," in *Proceedings of IEEE/RSJ International Conference on Intelligent Robots and Systems (IROS)*, Taipei, Taiwan, October 2010, pp. 5818 – 5823.